CHAPTER 4

Investigation of Repulsive Molecular Rydberg State

This chapter reports the experimental investigation and exploration of the adiabatic repulsive potential curve of Rb_2 in Rydberg state and the possibility of exploiting such interaction for the sake of single-atom loading technique. Section 4.1 describes the optical circuits designed for preparing the optical frequencies required for the Rydberg excitation and detection of rubidium-87. In this experiment atoms are initially cooled and trapped by the magneto-optical trap and then loaded into one-dimensional optical lattice before applying Rydberg excitation. Section 4.2 presents the diagnostic of atomic ensemble in the lattice. The strategy for investigation of repulsive interaction of Rb_2 and the experimental results are presented in section 4.3.

4.1 Experimental setup

The section details the optical setup of laser system required for operating the magneto-optical trap, one-dimensional optical lattice, and two-photon excitation of Rydberg states of rubidium-87 atom.

4.1.1 Magneto-optical trap lasers

Generation of a rubidium magneto-optical trap (MOT) requires two optical frequencies: MOT-cooling laser and MOT-repumping laser. The frequencies of these laser differ by 6.8GHz in rubidium-87. The optical schematics of cooling and repumping lasers are shown in Fig.(4.1) and Fig.(4.2) respectively. The cooling laser serves the optical frequencies for both MOT loading and MOT imaging processes. The whole laser system is based on phase lock technique using two the external cavity diode lasers (ECDL) with Littrow configuration. The output frequency of ECDL 0 is stabilized using standard saturated absorption spectroscopy and used as the reference frequency in phase locking. The frequency is locked with respect to the crossover peak $F = \mathrm{CO}(1,3)$ D2 line. ECDL 1

serves the main power of cooling laser using the tapered amplifier (TA). The output frequency of ECDL1 is stabilized with frequency of ECDL0 using the phase locking. The repumping laser is obtained from ECDL2 whose output frequency is locked at transition frequency $F = 1 \rightarrow F' = 2$.

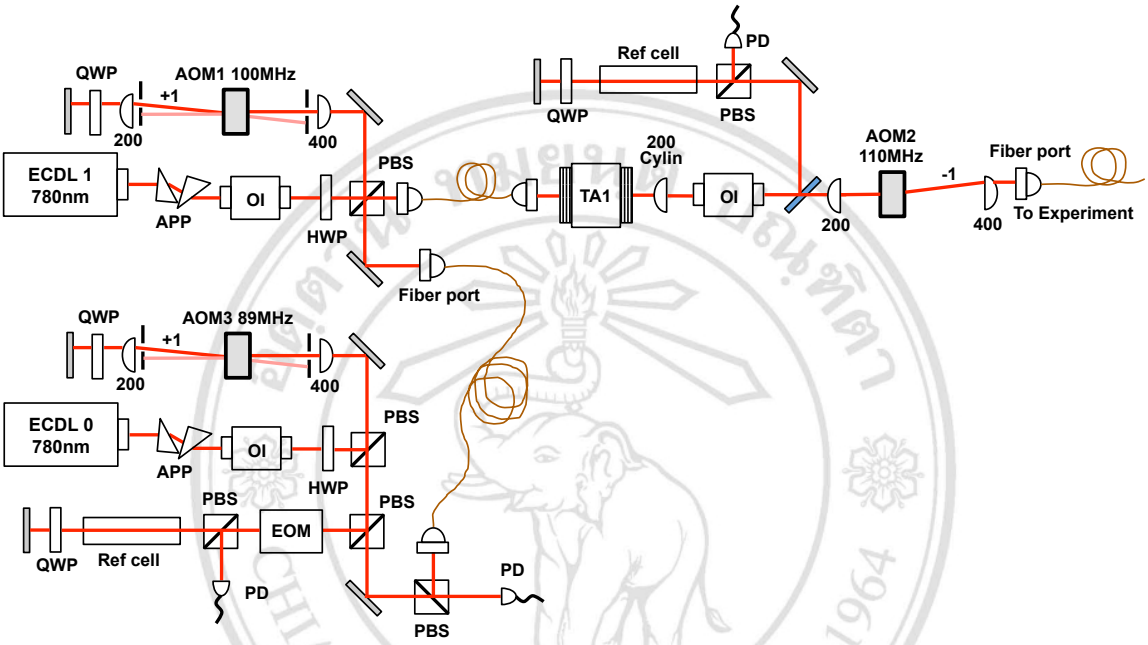

Figure 4.1: Optical schematic of MOT cooling laser. The phase locking technique is used to stabilize output frequency of ECDL1 with respect to ECDL0. The output power was amplified by the tapered amplifier. OI = optical isolator, HWP = haft-wave plate, QWP = quarter-wave plate, APP = anamorphic prism pair, PBS = polarizing beam splitter

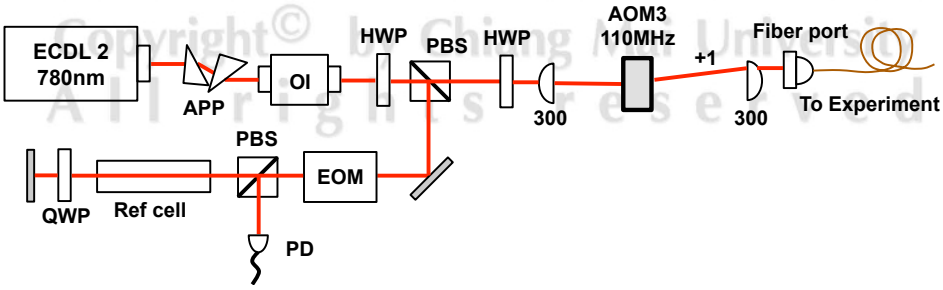

Figure 4.2: Optical schematic of MOT repumping laser.

4.1.2 Optical lattice laser

The lattice trap laser produces a laser beam for generating an one-dimensional optical lattice formed by the cavity in the chamber. In this experiment, the lattice laser is a homemade external cavity diode laser (ECDL3) operating at the wavelength of 808 nm. The laser was controlled via a homemade current controller and a homemade temperature controller. The dipole laser has a total optical output power of 100mW but due to the non-Gaussian profile the power much loss by coupling into a fiber. Hence the final power before going into the experiment is 9 mW. The frequency of laser was stabilized to a mode of tranfercavity using Pound-Drever-Hall technique. The schematic of optical setup around the lattice laser is shown in Fig.(4.3).

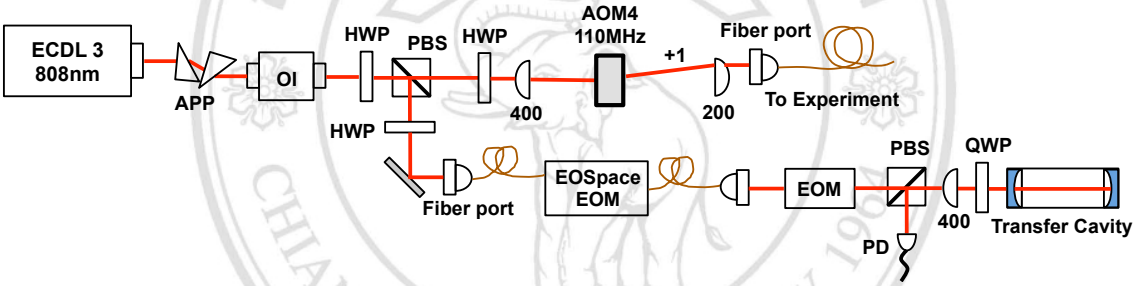

Figure 4.3: Optical schematic of optical lattice laser.

4.1.3 Probe laser

The optical schematic of probing lasers is shown in Fig.(4.4). The optical frequency used for the Rydberg excitation was derived from the external cavity diode lasers (ECDL 4) based on the Littrow configuration. ECDL 4 is a homemade laser system using an anti-reflection coated (AR) laser diode as a light source in order to avoid mode hopping. The output frequency is stabilized with the transfer cavity via a standard Pound-Drever-Hall configuration. In order to set the stabilized frequency with respect to transition frequency of rubidium-87. The computer controller AOM5 and EOSpace EOM were used to adjust the locked frequency according the the error signal obtained from the saturated absorption spectroscopy.

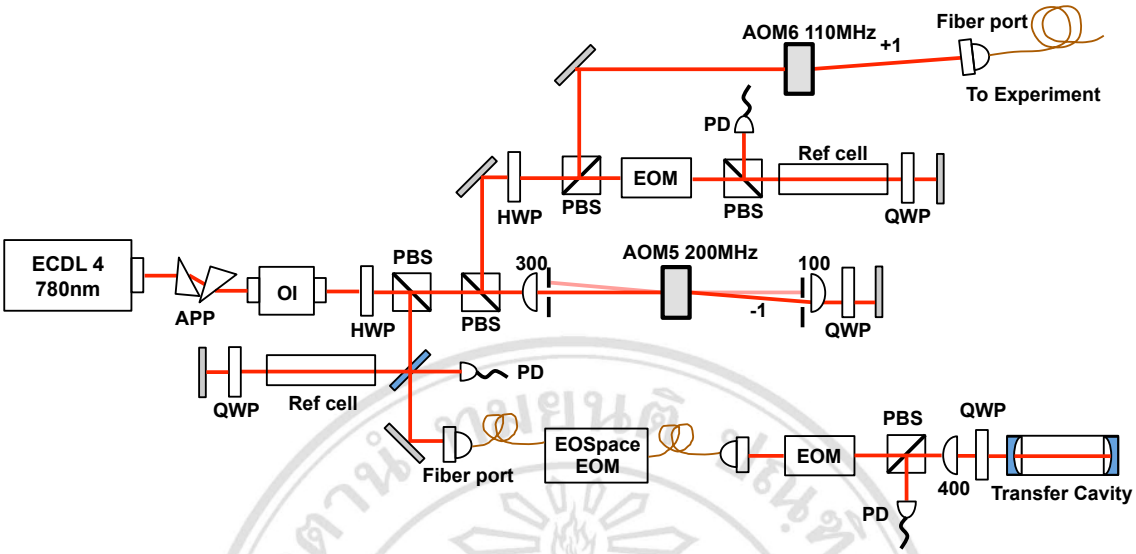

Figure 4.4: Optical schematic of probe laser for Rydberg excitation.

4.1.4 Coupling laser

Fig.(4.4) depicts the optical schematic of 480 nm laser. The laser serves the optical frequency used for two-photon transition of Rydberg state as the coupling laser. Since there is no available laser diode directly emits 480 nm light, a system of doubling frequency was exploited. The 960 nm laser (ECDL5) was used to produce 480nm light by coupling the 960nm light into the Bow-tie cavity containing the crystal used for produce doubled frequency photons. Due to low efficiency of doubling frequency creation. The tapered amplifier (TA2) was used to increase the overall output power of 480nm coupling light. The seed frequency of 960nm laser is stabilized with the transfer cavity using a standard Pound-Drever-Hall configuration. The frequency of coupling light is tuned can controller by computer-controlled EOSpace EOM.

4.1.5 Experimental geometry

Fig. (4.6) shows the experimental configuration used for study trap loss due to light-assisted cold collision between Rydberg atom and ground state atom. The one-dimensional optical lattice is formed by linear polarized 808nm wavelength light in high finesses cavity. The power of 808nm laser is 9 mW before going into the cavity and

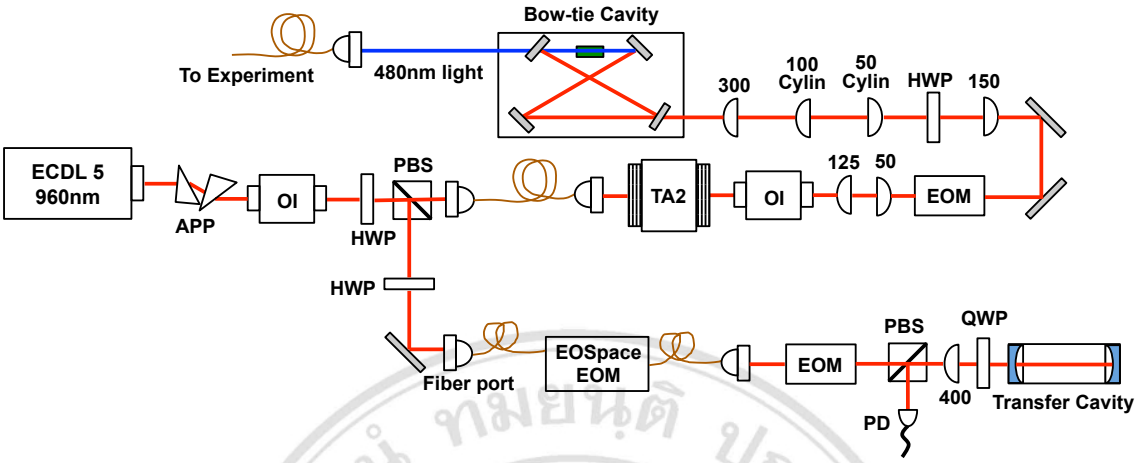

Figure 4.5: Optical schematic of coupling laser for Rydberg excitation.

this leads to the trap depth (total AC Stark Shift of $5^2S_{1/2}F = 1, 2$) of 7 MHz or 380 μK. The magnetic field of 6.5 G for defining a quantization axis is generated by a pair of Helmholtz coil. The field direction is downward, hence defines $+z$ axis direction. To measure trap loss, we perform atom number counting by absorption imaging method. The 780nm imaging beam is directed from the bottom pass through the lattice and then go to the camera. The imaging beam has σ^- polarization with respect to direction of magnetic field. In the same direction, there is a 780nm probe beam for applying two-photon transition. The 480nm coupling beam goes into the chamber in the same direction as 808nm dipole trap beam. This helps the coupling beam to interact with almost atoms in the lattice. Note that the linear polarization of the coupling beam is superposition of σ^+ and σ^- along the quantization axis. The MOT-repumping beam is setup to pass the lattice along y axis. Fig. (4.7) shows some parameters about the experiment.

4.2 One-dimensional optical lattice diagnosis

Since the nature of light assisted collision depends on many factors including average separation distance between two adjacent atoms, motional temperature of sample and the rate of excitation to a semi-molecular potential, the efficiency of single-atom loading also depends on such factors. Hence the atomic sample needs to be characterized in order to get necessary information needed for exploring the repulsive interaction between

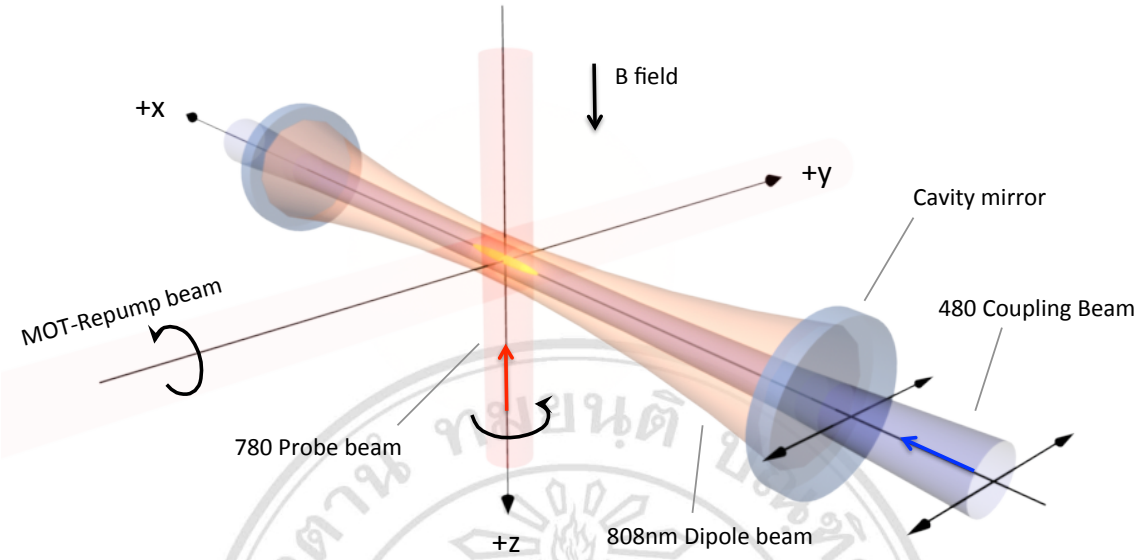

Figure 4.6: The configuration of laser beams used in the experiment: The red and blue arrows show propagation direction of 780nm probe beam and 480nm coupling beam respectively. The two double arrows on the right hand side represent linear polarization direction of 808nm dipole beam and the coupling beam respectively. MOT-repump beam propagates in $+y$ direction with circular polatization. The downward magnetic field B define quantization axis $+z$.

a Rydberg atom and a ground-state atom. The characteristics of atomic ensemble in the optical lattice including number of stored atoms, trap lifetime, density distribution, and temperature are presented in this section.

4.2.1 Trap lifetime of optical lattice

Under the vacuum condition operated in this work and in the absence of any laser light except the dipole laser, loss of trapped atoms in the optical lattice can occur by collision with thermal gases in the chamber. The rate of such collision determines the lifetime of atoms in the trap. Fig.(4.8) shows the measured number of stored atom decaying exponentially as function of time. Due to temperature fluctuation caused by the heated rubidium getter, the typical values of trap lifetime achieved in the experiment is limited to 580 ms.

Experimental Parameters

- MOT Beam Power (each) 30 mW
- Cavity Specification
  - Length 6.3 cm
  - Radius of curvature of cavity mirrors 10 cm
  - Diameter of cavity mirros 1.27 cm
  - Waist at 808 nm 109 μm
  - Rayleigh range 808 nm 4.6 cm
  - Finsees at 808 nm 3000
- 480nm Power (into chamber) 70 mW
- 480nm Waist (at clound) 40 μm
- 808nm Power (into chamber) 9 mW
- Magnetic field (quantization) downward
- Magnification (Imaging) 2.23
- 780 Probe Power 0.81 μW
- 780 Probe Waist 530 μm
- 780 Probe detuning form ($5^2P_{3/2}$) +100 MHz

Figure 4.7: Experimental parameters in Rydberg experiment

4.2.2 Temperature of optical lattice

Considering the thermal cloud of lattice and assuming that trapped atoms are in a thermal equilibrium where the Maxwell-Boltzmann static is valid, the temperature of cold atomic cloud can be determined from the free-space ballistic thermal expansion. The measurement begins by switching off the lattice beam. After a delay time τ, the camera shutter is opened and the probe beam is switched on and then an absorption image of atomic cloud is captured. Due to the cloud is distributed in a Gaussian profile, the standard deviation σ of the distribution can be extracted from the image. By varying the delay time and collecting the corresponding $\sigma(\tau)$, the temperature T can be calculated by apply a linear fitting to the equation [40]

$$\sigma^2(\tau) = \sigma_o^2 + \frac{k_B T}{m}\tau^2, \tag{4.1}$$

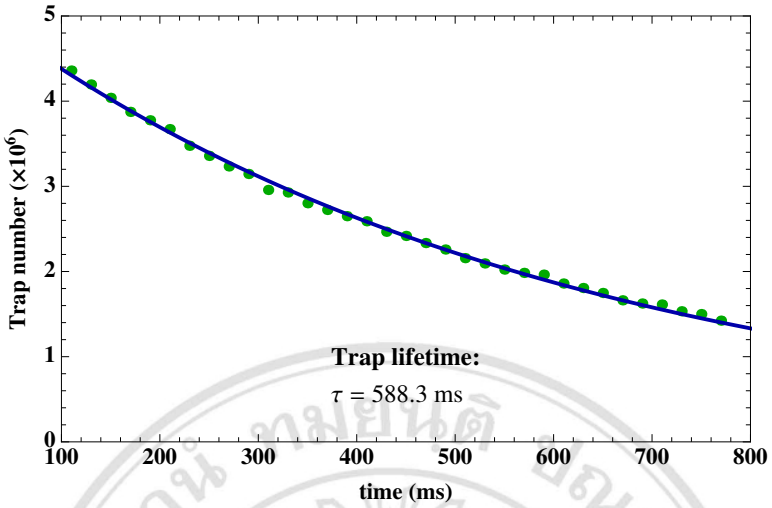

Figure 4.8: Measured trap lifetime of rubidium atoms in the optical lattice. Trap lifetime of 588.3 ms was obtained by fitting the data with exponential decay function.

where m is the mass of a rubidium atom in SI unit. The plot of squared standard deviation versus squared delay time is shown in Fig.(4.9) and the fit corresponds to a temperature of 65 μK. However the temperature gradually increases over time due to heating processes contributed by interaction with 808nm lattice laser.

4.2.3 Density distribution of optical lattice

According to the Maxwell-Boltzmann statistic, trapped atoms stored in an optical potential $U(\vec{\boldsymbol{r}})$ at equilibrium temperature T have density distribution $n(\vec{\boldsymbol{r}})$ given by

$$n(\vec{\boldsymbol{r}}) = n_o \exp\left(-\frac{U(\vec{\boldsymbol{r}})}{k_B T}\right), \tag{4.2}$$

where n_o is the peak density and $\vec{\boldsymbol{r}}$ is position vector. Trap potential of optical lattice can be approximated as the 3D harmonic potential that has cylindrical symmetry. Consequently, the density distribution of atomic cloud has Gaussian profile. Gaussian fit of the distribution along axial and radial directions are shown in Fig.(4.10). It should be noted that the distribution shown in the figure was obtained after letting atomic cloud ballistically expands for 1.5 ms before the images were taken. In order to find the true density distribution profile, the measured temperature and Eq.(4.1) are used to calculate

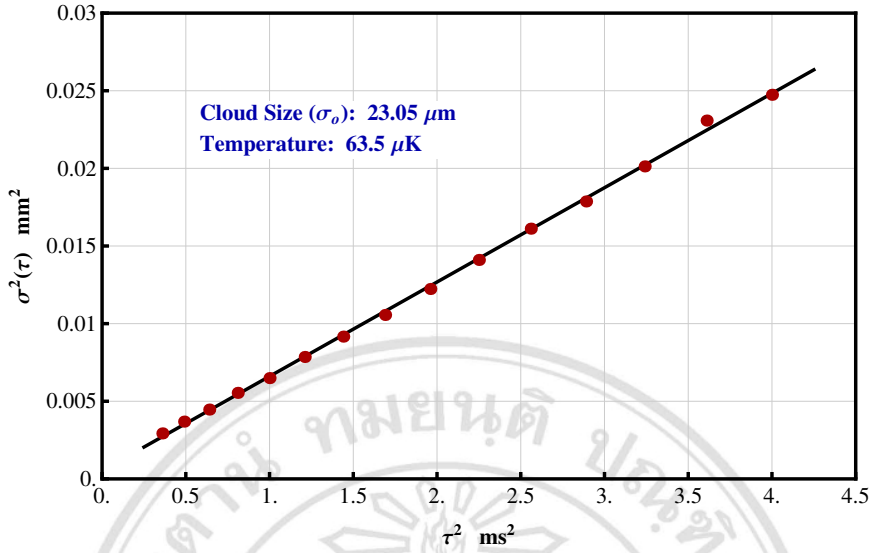

Figure 4.9: Temperature measurement by free-space ballistic expansion method. The data (red points) are fitted with Eq.(4.1).

initial standard deviation of Gaussian profile before releasing the trap. The distribution of number of stored atoms in each lattice site is shown in Fig.(4.11).

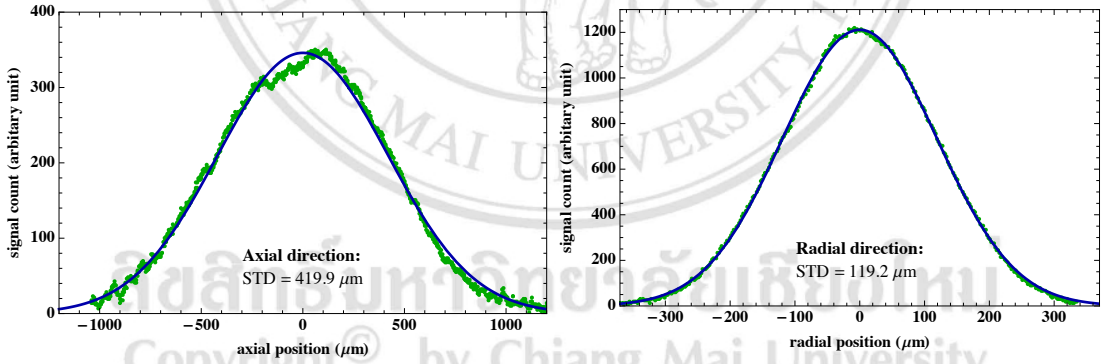

Figure 4.10: Gaussian fitted profile represents how position of trapped atoms are distributed in the trap. The signal count data were obtained from converting the absorption image of atomic cloud Fig.(4.18)(right).

In a single lattice site, the standard deviation of atomic cloud distribution along the axial direction is much smaller than the typical range of interaction between a Rydberg atom and a ground-state atom. The density distribution appropriated for this work is represented in 2D.

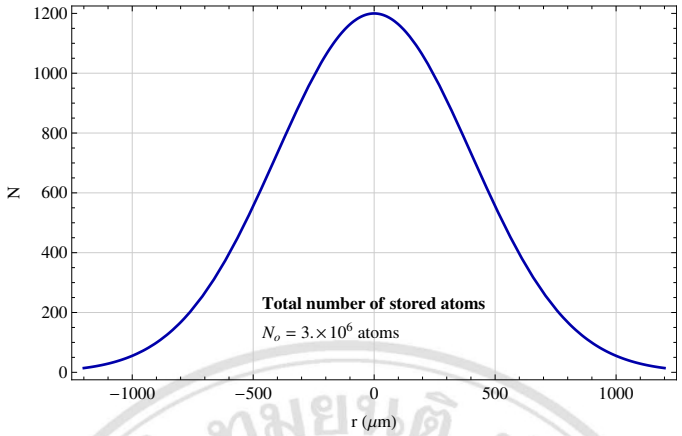

Figure 4.11: The distribution of number of trapped atom along cavity axis.

4.3 Trap loss due to blue-detuned two-photon excitation

This section details the experimental procedure to investigate and explore the possibility of exploiting a repulsive interaction between a Rydberg rubidium atom and a ground-state atom. In order to confirm the existence of a repulsive Rydberg-ground interaction that has a practical capability of supporting our mechanism, the trap loss measurement due to blue-detuned Rydberg excitation needs to be performed. There are two types of measurement presented in this work.

4.3.1 Trap loss as function of detuning

The first type of this measurement is done by comparing the number of atoms remaining in the trap before and after applying the Rydberg excitation lasers whose optical frequency is varied across the resonance frequency. Basically, the probability of trap loss would be maximum when the optical frequency of excitation light is resonant with Rydberg transition frequency and it decreases when the frequency of the laser is off the resonance.

4.3.2 Trap loss at fixed detuning

The second type of trap loss measurement is performed by fixing the detuning above the one-body excitation resonance. Then the remaining number of stored atom is plotted as function of probing time.

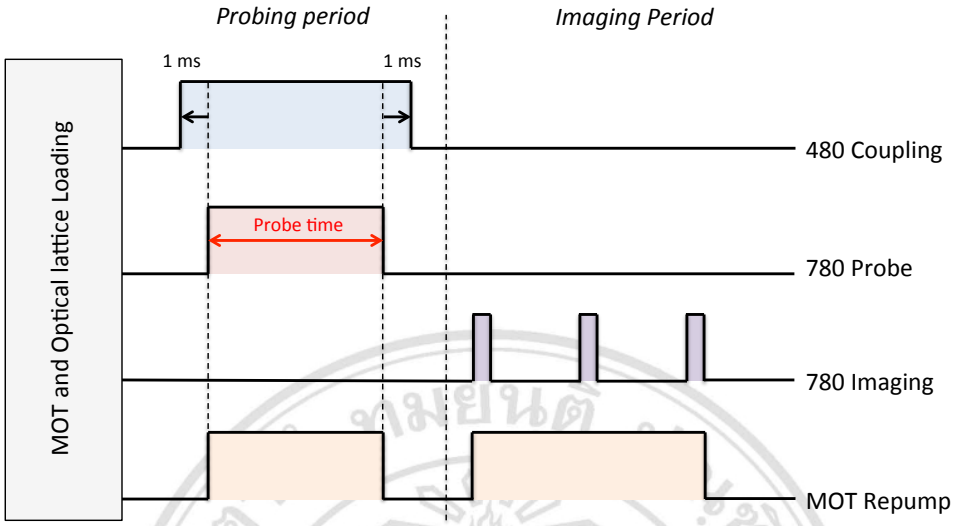

Figure 4.12: Time sequence of experiment: The 480nm coupling beam is turned on 1ms before 780nm probe beam to avoid trap loss due to 780nm light. MOT-repumping beam is also turned on over the probing period. This helps to pump atoms that decays from the Rydberg state to $5^2S_{1/2}F = 1$ go back to $5^2S_{1/2}F = 2$ for next Rydberg excitation.

4.3.3 Time sequence and results

The time sequence of the experiment is shown in Fig. (4.12). The cold atomic ensemble is initially prepared from standard magneto optical trap (MOT) while the optical lattice is turned on. This produces dark magneto optical trap with low temperature. After MOT loading period, the intensity of MOT beams is then decreased and its detuning (from $5^2S_{1/2}F = 2 \rightarrow 5^2P_{3/2}F' = 3$) is gradually changed from -18 MHz to -185 MHz for performing sub-Doppler cooling. The cloud after this cooling process has temperature of 65 μK. In the probing period, the 480nm coupling beam is turned on 1ms before 780nm probe beam for preventing any trap loss due to 780nm light. The detuning and power of the probe beam is fixed at blue-detuning +100 MHz from the intermediate state, $5^2P_{3/2}$ see Fig (4.13), and 0.8 μW respectively. This corresponds with the Rabi rate of 0.8 MHz. The detuning of the 480nm coupling beam is varied from 0 MHz to 20 MHz with respect to the effective bare transition ($5^2S_{1/2} \rightarrow 50^2S_{1/2}$ and no AC Stark Shift). The coupling beam has power of 70 mW and this corresponds with the effective two-photon transition rate of 54 kHz, $\Omega = \Omega_1\Omega_2/(2\Delta)$. The Fig. (4.14-4.17) show the measured number of

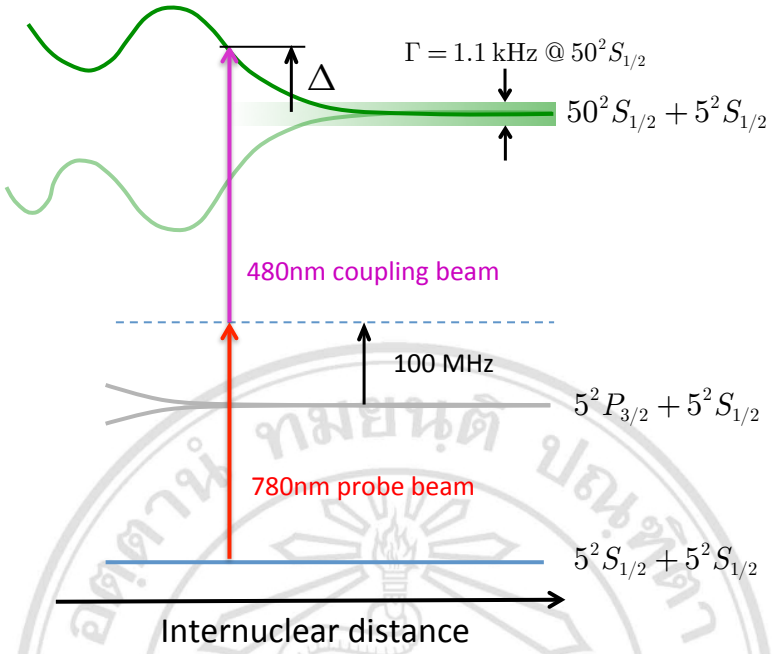

Figure 4.13: Excitation Scheme of Rydberg experiment: the energy levels presented here are bare states, no AC Stark shift.

trapped atom as function of detuning Δ for 100 ms and 20 ms probing time. For imaging period, the 780nm imaging beam is derived from the MOT beam with detuning of -2.2 MHz from $5^2S_{1/2}F = 2 \rightarrow 5^2P_{3/2}F = 3$ transition. The pulse length of imaging beam is 100 μs and the optical lattice is tuned off 1.5 ms before taking images. This trap dropping releases the cloud expanding and hence reduces the optical density of atomic cloud. This improves efficiency of trapped atom counting. There are three images taken in the detection process; with atom, without atom, and background. These images are taken with 35 ms apart from each other. To extract the number of trapped atoms, the background is subtracted from the first two images and then the second image is subtracted from the first image. The trap number is given by integration over the area of atomic cloud. Fig. (4.18) shows an example of atomic cloud image after subtraction.

4.4 Summary and outlook

Up to present, we have performed theoretical analyses, numerical calculations and experiment for investigating whether or not the Rydberg-ground repulsive adiabatic po-

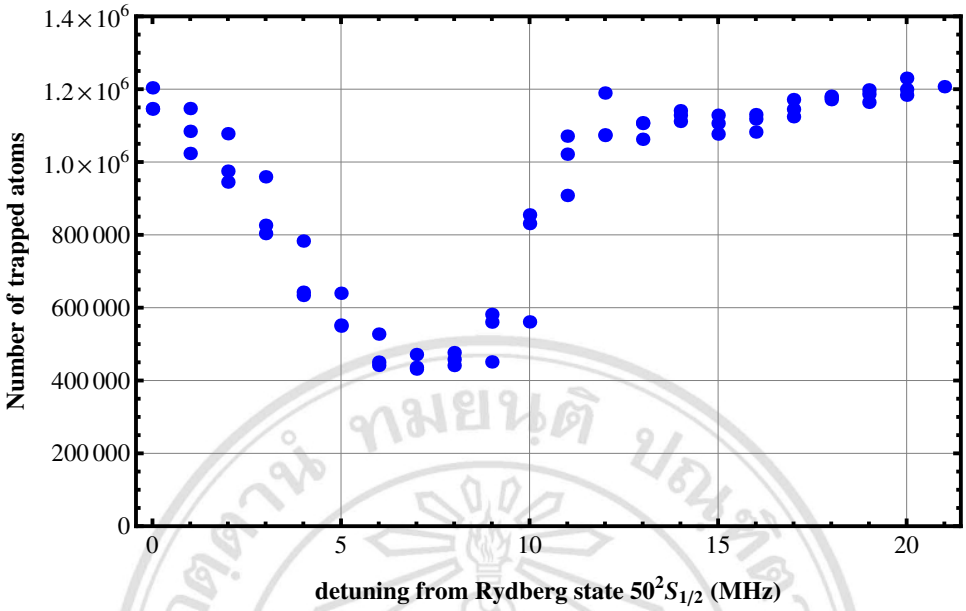

Figure 4.14: Number of remaining trapped atom after 100 ms of probing time as function of detuning Δ from Rydberg state $50^2S_{1/2}$. The lowest dip at 7 MHz shows trap loss due to on-resonance Rydberg excitation compensated with AC Stark shift of ground state $5^2S_{1/2}$. The other small dip at 15 MHz shows trap loss due to blue-detuning excitation.

tential energy have strong enough potential for leading to the deterministic single-atom loading in an optical micro-trap. In the future, we are looking for the scalable single-atom source on demand based on this technique and also the discussion of combination with the collisional blockade.

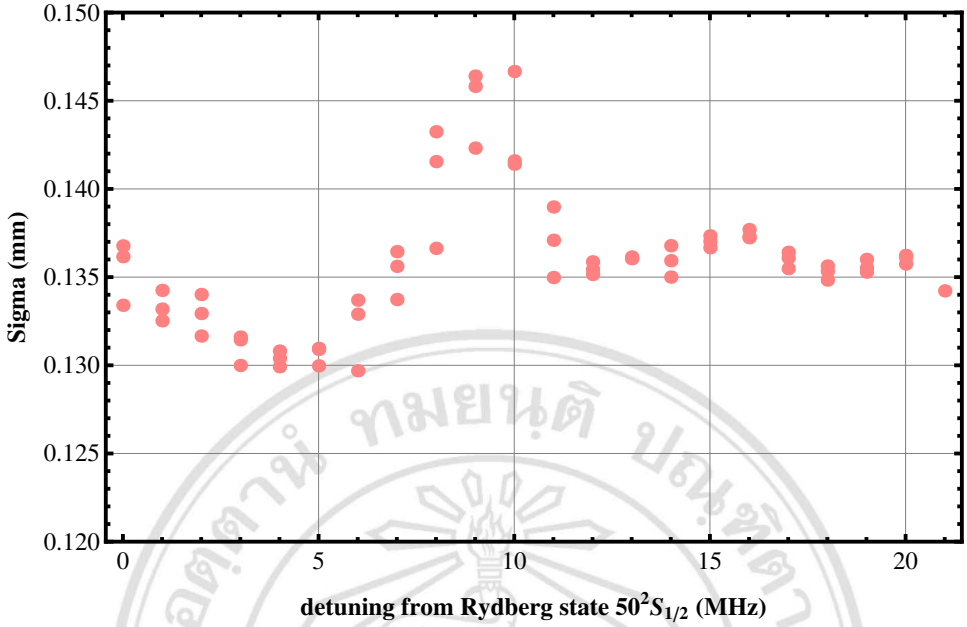

Figure 4.15: This plot shows the standard deviation of atomic cloud Gaussian fitting after 100 ms probing time. At 15 MHz detuning it shows heating (increase in cloud size) due to blue-detuning Rydberg excitation.

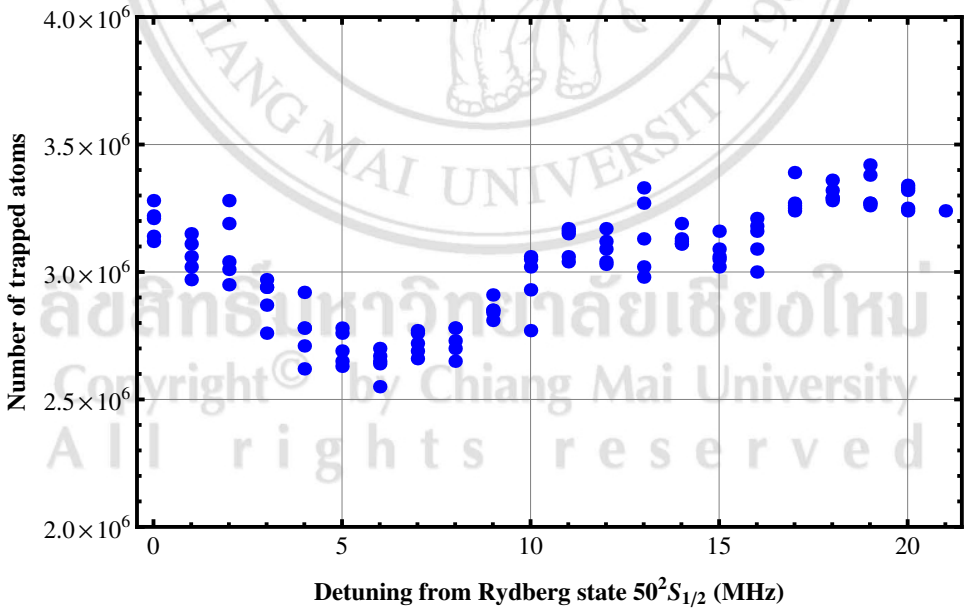

Figure 4.16: Number of remaining trapped atom after 20 ms of probing time as function of detuning Δ from Rydberg state $50^2S_{1/2}$. The lowest dip at about 6 MHz shows trap loss due to on-resonance Rydberg excitation compensated with AC Stark shift of ground state $5^2S_{1/2}$. The next small dip at 15 MHz shows the trap loss due to blue-detuning excitation.

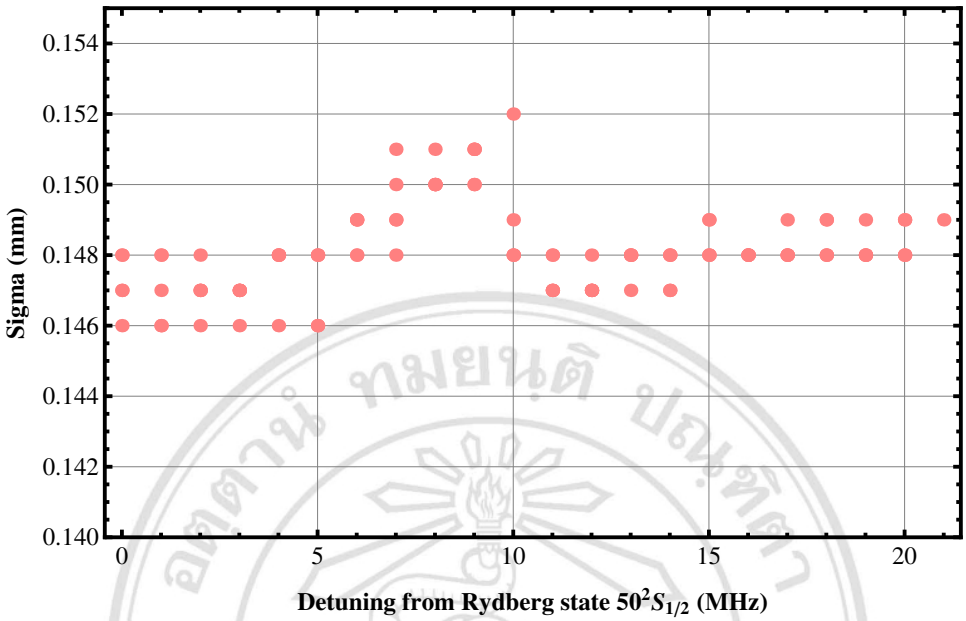

Figure 4.17: This plot shows the standard deviation of atomic cloud Gaussian fitting after 20 ms probing time. At 15 MHz detuning it does not show cleary heating because short excitation time.

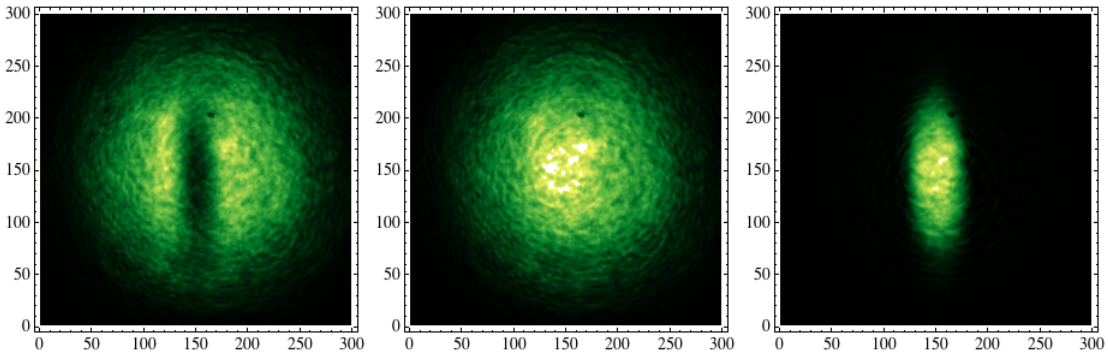

Figure 4.18: In imaging process, the first image (left) is taken while trapped atom are released 1.5ms before taking image and expanding ballistically. The second image (center) is taken after waiting until there is no atoms in the area of imaging. Theses images are subtracted from each other for getting the cloud of atom in the lattice (right). The raw images have resolution of 2048x2048 pixels. Gaussian resmapling method is used to reduce the resolution down to 512x512 pixels. The totoal number of trapped atom is 3 million.